Response of the Osmotic Tensiometer to Varying Temperatures: Modeling and Experimental Validation

P. Maarten Biesheuvel, Ron Raangs, and Henk Verweij*

ABSTRACT

In an osmotic tensiometer, the hydrostatic pressure of a confined polymer solution is measured to infer the soil water potential. Essential in the operation is the osmotic potential of the polymer solution. Because the osmotic potential depends on the temperature, a significant and undesired *pressure lag* may develop when the osmotic tensiometer is used under conditions of varying temperature. To understand and eliminate the pressure lag, a dynamic transport model was derived that describes the time response of the osmotic tensiometer while assuming complete temperature equilibration and a resistance to water transfer that is fully located within the filter. Essential elements of the model are the filter conductance and the sensitivity of the pressure transducer, for which submodels are set up. The transport model is validated with measurements on an osmotic tensiometer that uses an inorganic membrane as filter. The experiments were done for instrument-limited conditions by placing the osmotic tensiometer in free water. For these conditions, the model describes measurements with reasonable accuracy. The new transport model clarifies the behavior of the osmotic tensiometer for changing temperatures and can be used to design an osmotic tensiometer with a lower pressure lag.

THE IN SITU AND DIRECT MEASUREMENT OF SOIL WATER POTENTIAL is still far from straightforward. Existing methods, such as the gypsum block, the conventional tensiometer, and the high-range suction sensor, have the disadvantages of slow response (gypsum block), small measurement range (conventional tensiometer; Bocking and Fredlund, 1979), or decreasing pressure in time due to evaporation from the ceramic filter, especially in soils with a low degree of saturation (high-range suction sensor; Guan and Fredlund, 1997). Also, cavitation occurs in a conventional tensiometer if the dry end of its range is reached.

To obviate the disadvantages of the conventional tensiometer, Peck and Rabbidge (1966, 1969a, b) first used a concentrated polymer solution inside the conventional tensiometer in order to measure the soil water potential for a much increased range. This *osmotic* tensiometer has the additional advantage that, after reaching the dry end of the measurement range, it can be recovered completely by bringing it into contact with free water. The osmotic tensiometer was used by Bocking and Fredlund (1979), who concluded that many difficulties stand in the way of a routine application of the osmotic tensiometer. First, polymer retention by the filter was not 100%, and hence, the osmotic tensiometer readings changed in time while the measurement range decreased. Secondly, the osmotic tensiometer had a slow response on changing temperature and soil water potential. Thirdly, these researchers argued that the influence of the temperature on the osmotic potential of the polymer solution limits application of the osmotic tensiometer to temperature-controlled laboratory experiments.

We have developed an osmotic tensiometer that may overcome these difficulties (Fig. 1). In our version, a porous inorganic filter is used that consists of a thick support layer and a thin microporous membrane. These inorganic membranes are durable in any environment (De Vos and Verweij, 1998), and for large polymers (e.g., mol. wt. > 20 kg mol^{-1}), polymer retention was close to 100% for a long period. The response time can be minimized for an osmotic tensiometer by combining a permeable filter with a stiff housing, a small cell volume, and a sensitive pressure transducer. Finally, the influence of temperature on the osmotic potential can be substituted readily in the pressure transducer software used to read the osmotic tensiometer pressure, which enables the use of the osmotic tensiometer under field conditions.

The γ-alumina membranes used in our osmotic tensiometer may prevent ions in the soil from entering the tensiometer cup (Alami-Younssi et al., 1995). If ions are indeed rejected completely by the membrane, then the tensiometer will measure the total soil water potential; however, if ions permeate the filter freely, then the tensiometer measures the matric potential of the soil. In this work, no attention is paid to this difference because it is yet unknown to what extent ions are rejected by our membranes. Furthermore, in the experiments in this paper, distilled water is used to simulate the soil environment, and for these experiments the total soil water potential equals the matric potential. So, the term *soil potential* is used in this paper to describe the potential outside the osmotic tensiometer cup.

In this paper, we focus on the influence of (diurnal) temperature changes on the performance of the osmotic tensiometer because the osmotic potential of the polymer solution depends on its temperature. Haise and Kelley (1950) and Watson and Jackson (1967) also studied the influence of diurnal temperature changes on conventional tensiometer performance. Haise and Kelley (1950) ascribed this influence to the transfer of water vapor to locations of lower temperature, while Watson and Jackson (1967) attributed the pressure change to the expansion of the tubing used to connect the conventional tensiometer to the pressure transducer. Putting aside the effects described by these researchers, the present paper will discuss only the influence of temperature on the osmotic potential of the polymer solution.

Because of temperatures changes (e.g., due to the

P. Maarten Biesheuvel and Henk Verweij, Lab. for Inorganic Materials Sci., Dep. of Chem. Technol. and MESA Res. Inst., Univ. of Twente, P.O. Box 217, 7500 AE Enschede, the Netherlands; and Ron Raangs, Dep. of Environ. Sci., Subdep. Water Resour., Wageningen Univ., Nieuwe Kanaal 11, 6709 PA Wageningen, the Netherlands. Received 28 Aug. 1998. *Corresponding author (h.verweij@ct.utwente.nl).

Published in Soil Sci. Soc. Am. J. 63:1571–1579 (1999).

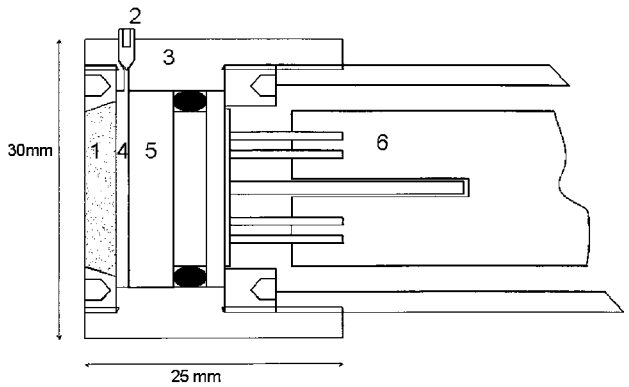

Fig. 1. Construction of osmotic tensiometer: 1, ceramic filter; 2, injection point; 3, brass housing; 4, cell filled with polymer–water solution; 5 pressure transducer; 6, data transfer.

diurnal cycle) and its effect on the osmotic potential of the polymer solution inside the osmotic tensiometer, water is forced to move through the filter. As the conductance of the filter is finite, a pressure lag is introduced in the system, which can be considered a measurement error. It is the objective of this work to construct and validate a transport model that describes the influence of the important parameters (e.g., filter conductance and temperature gradients) on the magnitude of the pressure lag. The model may be useful in the design of osmotic tensiometers with reduced pressure lag.

THEORY

In this section, three key issues are covered. First, the assumptions that are made in the development of the transport model for the behavior of the osmotic tensiometer are summarized. Second, equations are developed for two important elements of the transport model, namely conductance and sensitivity. The final equation for the conductance is used in the Materials and Methods section, and the equations for the sensitivity are used in the Results and Discussion section. The third issue involves expressions that have been developed for the response behavior of conventional and osmotic tensiometers. Two cases are discussed for the conventional tensiometer in which the concept of pressure lag is introduced. In subsequent cases, the osmotic tensiometer is discussed for situations of increasing complexity. Calculations based on the last case will be compared with experiments in Results and Discussion.

Constraints of the Model

To describe the time response of the osmotic tensiometer, a transport model has been set up that is based on the following assumptions:

1. Temperature equilibration (heat transfer) with the surrounding soil and within the osmotic tensiometer is relatively rapid when compared to the transport of water. Temperature profiles are thus considered flat in the entire system.
2. Differential expansion of the liquid within the cell compared with that of the surrounding metal–ceramic housing does not induce an extra pressure change.
3. Expansion of the cell and housing at a higher pressure or temperature is low (stiff housing, incompressible liquid) and, therefore, does not influence the polymer concentration in the cell (Peck and Rabbidge, 1969a) nor the amount of water that needs to be transported into or out of the cell.
4. The osmotic potential of the liquid within the cell is only a function of the initial polymer concentration, the polymer type, the temperature, and the pH. The concentration of polymer in the cell remains constant because loss of polymer through the filter is negligible.
5. The resistance to water transfer into and out of the tensiometer cell is fully located within the filter; i.e., the soil is not limiting the transport velocity. This assumption appeared logical in the laboratory experiments described in the present paper, but it may be invalid under field conditions. In that situation, additional resistance can be present in the soil layer adjacent to the tensiometer or even in a small air gap between soil and tensiometer. Especially when the water phase in the soil becomes discontinuous and water transfer has to proceed by ordinary diffusion through the gas phase instead of through the liquid phase (e.g., Bird et al., 1960), resistance to water transfer in the soil outside the tensiometer may become extremely high. Inside the filter, the water is contained in a matrix of polymer, through which it must be transported, and when a layer of polymer is built up against the filter, resistance to transport because of the polymer may become high as well (Mulder, 1991).
6. Peck and Rabbidge (1969a) describe the detrimental effect of the development, adjacent to the filter, of a thin layer of solution that has a concentration different from that in the bulk of the cell. Equilibrium in the osmotic potential is then reached only when the osmotic solution has homogenized by diffusion. These effects are neglected in the model.

The model that will be discussed for the osmotic tensiometer resembles models developed previously for conventional tensiometers by Klute and Gardner (1962), who described tensiometer response when the soil potential changes gradually; and by Towner (1980), who investigated under which conditions the soil or the tensiometer resistance is limiting to water transfer.

Filter Conductance

The filter conductance K ($m^3\ s^{-1}\ Pa^{-1}$) is equal to the liquid flow (Φ_{vol}, $m^3\ s^{-1}$) per unit of potential difference across the filter (Pa). It depends on the intrinsic permeability L_i (m^2) of the filter materials used, the dimensions of the cup (thickness, form, surface area), and the viscosity of the liquid η (Pa s). If more than one material is used (e.g., a membrane on top of a porous support), then two resistances to flow are in series, and thus, the permeability L_i of each layer will come into play.

The permeability L_i is a material property and several expressions exist for the relationship between the structure of a material and its permeability. A well-known expression is the Carman-Kozeny equation for a packed bed of equally sized spheres (Dullien, 1979):

$$L_i = \frac{\varepsilon^3 r_p^2}{45(1-\varepsilon)^2} \quad [1]$$

Here, ε is the porosity of the material (volume fraction available for flow), and r_p is the particle radius. The coupling of L_i and K is based on Darcy's law for flow through a porous medium (Bird et al., 1960; Dullien, 1979):

$$J_{vol} = -\frac{L_i}{\eta}\frac{d\psi}{dr} \quad [2]$$

and the equation of continuity for stationary conditions:

$$0 = -r^{-\sigma}\frac{d}{dr}(r^{\sigma}J_{vol}) \quad [3]$$

Here, J_{vol} stands for the volume flux of liquid (m s^{-1}), ψ for the potential for water transfer (e.g., pressure or osmotic potential, Pa = J m^{-3}), and σ for the geometry ($\sigma = 0$ plan-parallel, $\sigma = 1$ cylindrical, and $\sigma = 2$ spherical); r is the space coordinate. In Eq. [3], it is assumed that within the filter liquid flows unidirectionally. Conductance K is given by the following definition (Richards et al., 1937; Richards, 1949):

$$K = \frac{\Phi_{vol}}{\Delta\psi} \quad [4]$$

Here, $\Delta\psi$ is the potential difference across the filter. From solution of Eq. [2] and [3] and comparison with Eq. [4], it follows that for a flat filter ($\sigma = 0$, plan-parallel geometry) K and L_i are related by

$$K = \frac{A\,L_i}{\eta\delta_f} \quad [5]$$

Here, A stands for the surface area available for liquid transport and δ_f for the thickness of the filter. Next, an example of a cylindrical cup with a rounded bottom is elaborated together with an example of the conductance of a filter that consists of more than one layer of different materials. The first geometry is often used for tensiometer cups, while the latter is used in this paper.

Conductance of a Porous Cup

An expression is derived for conductance K of a cylindrical cup of one type of material with a rounded bottom, as often used in tensiometers (Fig. 2). The permeabilities of the spherical cap and the cylindrical tube can be summed to give

$$K_{cup} = K_{cap} + K_{cyl} \quad [6]$$

Solution of the mass balance Eq. [3] for the half-sphere (cap) results in

$$\Phi_{vol} = J_{vol}2\pi r^2 \quad [7]$$

Substitution of Eq. [7] in Eq. [2], integration from ψ_1 at r_1 to ψ_2 at r_2, and substitution in Eq. [4] produces

$$K_{cap} = \frac{2\pi L_i}{\eta}\left(\frac{1}{r_1} - \frac{1}{r_2}\right)^{-1} \quad [8]$$

A similar derivation can be made for the cylindrical part, after which the total cup-conductance K_{cup} is given by

$$K_{cup} = \frac{2\pi L_i}{\eta}\left((r_1^{-1} - r_2^{-1})^{-1} + H\left(\ln\frac{r_2}{r_1}\right)^{-1}\right) \quad [9]$$

Conductance of Two-Layer Filter

If a filter is used consisting of more than one layer of a different permeability L_i, then a typical *resistances-in-series* expression is obtained. For plan-parallel geometry and for two layers, the following result is then obtained:

$$K = \frac{A}{\eta}\left(\frac{\delta_1}{L_1} + \frac{\delta_2}{L_2}\right)^{-1} \quad [10]$$

where δ_1 and δ_2 refer to the layer thicknesses, and L_1 and L_2 to the layer permeabilities.

Pressure Transducer Sensitivity

In this section, focus is on the sensitivity of the pressure transducer mounted in the osmotic tensiometer. Only if the expansion of the tensiometer cell by other means is low enough (e.g., by using a stiff housing or a small cell volume), can the transducer sensitivity be related directly to the overall tensiometer sensitivity.

The sensitivity is generally defined by (Richards, 1949)

$$S = \frac{dP}{dV} \quad [11]$$

Here, V stands for the volume of the cell and P for the

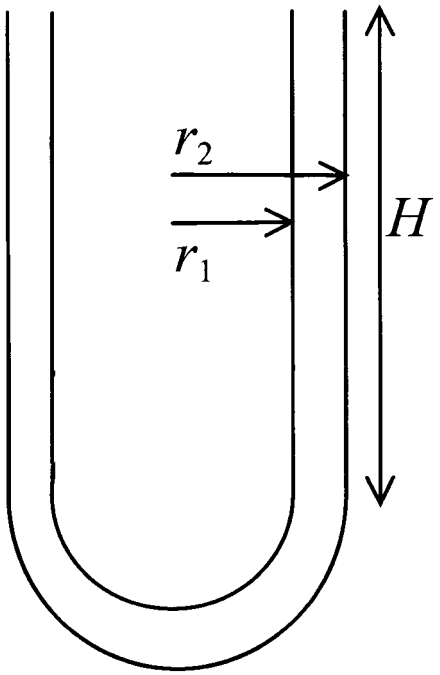

Fig. 2. Dimensions of typical tensiometer cup.

pressure within the cell. A typical sensitive pressure transducer consists of a thin, flexible, circular silicium wafer with a strain gauge inserted and glued onto a small cylindrical glass tube. The transducer is modeled as a clamped cylindrical plate with radius R and thickness δ_t that deforms under bending stresses (Fig. 3). The material is assumed to be isotropic and linearly elastic. For a thin disk ($\delta_t/R < 0.1$) and a low indent ($w_{r=0}/\delta_t < 0.1$), the indent r is then given by (Vinson, 1974) as

$$w = \frac{3P(1 - \nu^2)}{16E\delta_t^3}(R^2 - r^2)^2 \quad [12]$$

Here, ν stands for Poisson's ratio and P for the pressure difference between the cell and the reference state behind the transducer (e.g., atmospheric). After integration, the overall volumetric indent ΔV is given by

$$\Delta V = \int_0^R w(r)2\pi r dr = \frac{\pi P R^6(1 - \nu^2)}{16E\delta_t^3} \quad [13]$$

The sensitivity, S, is given by writing Eq. [13] in a differential form and substitution in Eq. [11]:

$$S = \frac{16E\delta_t^3}{\pi R^6(1 - \nu^2)} \quad [14]$$

According to Eq. [14], transducer sensitivity S is not dependent on the actual pressure difference, which is an advantage when these transducers are used in a tensiometer.

Time Response Behavior

Five cases are discussed that describe the behavior of the conventional and the osmotic tensiometer. In all cases it is assumed that conductance K and sensitivity S are constant. The soil potential is described as ψ_s and the potential in the tensiometer by ψ_T. For a conventional tensiometer, ψ_T only consists of a (static) pressure term and is replaced by P. For the osmotic tensiometer, ψ_T is the sum of the osmotic potential ψ_o and pressure P.

In that case, Eq. [4] results in (Bocking and Fredlund, 1979)

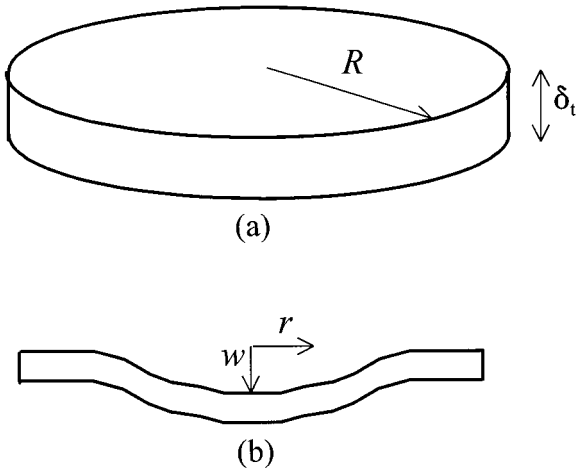

Fig. 3. Pressure transducer (a) without pressure difference and (b) flexed due to pressure difference.

$$\Phi_{vol} = K(\psi_T - \psi_s) = K(P + \psi_o - \psi_s) \quad [15]$$

Case 1. Step Change in Potential for a Conventional Tensiometer

For a conventional tensiometer, Eq. [15] simplifies to

$$\Phi_{vol} = K(P - \psi_s) \quad [16]$$

Flow Φ_{vol} is also given by

$$\Phi_{vol} = -dV/dt \quad [17]$$

where t refers to time (s). The pressure change is given by

$$\frac{dP}{dt} = \frac{dP}{dV}\frac{dV}{dt} \quad [18]$$

Substitution of Eq. [11], [16], and [17] in Eq. [18] results in

$$\frac{dP}{dt} = -SK(P - \psi_s) \quad [19]$$

Integration with initial condition $P|_{t=0} = P_0$ results in

$$P = \psi_s + (P_0 - \psi_s)e^{-SKt} \quad [20]$$

If the tensiometer is at equilibrium with the surrounding soil for $t < 0$, then $\psi_{s,0} = P_0$. If at $t = 0$ soil potential is changed step-wise from $\psi_{s,0}$ to ψ_s, then the change of P from P_0 is described by Eq. [20]. The response time is defined as the time necessary for the driving force ($P - \psi_s$) to be reduced to 1/e times the original driving force ($P_0 - \psi_s$), which is, according to Eq. [20] (Richards, 1949),

$$\tau = \frac{1}{KS} \quad [21]$$

For the driving force to be reduced by 99% (which may be a criterium for reaching equilibrium) time t must equal 4.6τ. This analysis clearly shows that for a step-change in soil potential, permeability K and sensitivity S are equally important for the response time of a conventional tensiometer. The difference between P and ψ_s is called the pressure lag, PL_{CT}, which is the measurement error introduced by the lag of the conventional tensiometer (see also Klute and Gardner, 1962, Eq.[7]). Because a measurement error is usually specified as a positive number, the absolute value is used. According to Eq. [20], the pressure lag for a conventional tensionmeter is given by

$$PL_{CT} = |(P_0 - \psi_s)e^{-SKt}| \quad [22]$$

The pressure lag, PL_{CT}, decreases in time and will finally become zero.

Case 2. Gradual Potential Change for a Conventional Tensiometer

If the soil potential is not constant, but changes in time, then Eq. [19] cannot be solved as done in Case 1. If the soil potential changes linearly in time, the following equation holds:

$$\psi_s = \psi_{s,0} + \delta t \quad [23]$$

Here, the change of soil potential with time δ is given by

$$\delta = \frac{d\psi_s}{dt} \quad [24]$$

Equation [19] changes to

$$\frac{dP}{dt} = -SK(P - \psi_{s,0} - \delta t) \quad [25]$$

Integration of Eq. [25] with initial condition $P|_{t=0} = P_0$ results in

$$P = \psi_{s,0} + \delta t - \frac{\delta}{SK}(1 - e^{-SKt}) + (P_0 - \psi_{s,0})e^{-SKt} \quad [26]$$

If the conventional tensiometer was at equilibrium with the soil initially; i.e., $P_0 = \psi_{s,0}$; the pressure lag PL_{CT} is given by

$$PL_{CT} = \left|\frac{\delta}{SK}(1 - e^{-SKt})\right| \quad [27]$$

If Eq. [27] is compared with Eq. [22], then it becomes clear that in case of a gradual change of soil potential, the tensiometer will always lag behind and PL_{CT} will increase in time; whereas for a step-change, PL_{CT} will decrease and eventually become zero.

Case 3. Gradual Potential Change for an Osmotic Tensiometer

The gradual change in soil potential, as defined by δ, can easily be as low as 100 cm H_2O d^{-1} (0.12 Pa s^{-1}) or less. In that case, another effect can become more pronounced for an *osmotic* tensiometer: namely, the change in osmotic potential of the polymer solution in the cell because of the changing temperature of the soil, T, during day and night. To calculate this, two parameters must be defined: the rate of temperature change, α [K s^{-1}],

$$\alpha = \frac{dT}{dt} \quad [28]$$

and the change of osmotic potential with temperature, β [Pa K^{-1}],

$$\beta = \frac{d\psi_o}{dT} \quad [29]$$

To determine the main cause of potential change in the system, δ must be compared with the product $\alpha\beta$. For $\alpha = 2.3 \times 10^{-4}$ K s^{-1} and $\beta = 3.75 \times 10^4$ Pa K^{-1} (see Results and Discussion), the product $\alpha\beta$ has a value of 8.6 Pa s^{-1}, which is roughly seventy times the value for δ given above.

For reasons of simplicity, the influence of temperature on the soil potential ψ_s is neglected in the remainder of this paper even though this influence can be significant, especially in drier soils (see Campbell and Gardner 1971; Liu and Dane, 1993). If β is considered constant as well, the change of osmotic potential with temperature follows from integration of Eq. [29]:

$$\psi_o = \psi_o^* + \beta(T - T^*) \quad [30]$$

Here, (T^*, ψ_o) is an arbitrary reference point chosen to linearly describe ψ_o, and it is not necessarily similar to initial temperature T_0 or initial osmotic potential $\psi_{o,0}$. If temperature changes continuously (i.e., α is constant), then Eq. [28] can be integrated starting from the initial temperature T_0 at $t = 0$. Substitution in Eq. [30] results in

$$\psi_o = \psi_o^* + \beta(T_0 + \alpha t - T^*) \quad [31]$$

Substitution of Eq. [11], [15], [17] and [32] in Eq. [18] results in

$$\frac{dP}{dt} = -SK(P + \psi_o^* + \beta(T_0 + \alpha t - T^*) - \psi_s) \quad [32]$$

Solution of Eq. [32] with initial condition $P|_{t=0}$ results in

$$P = \psi_s - \psi_o^* - \beta(T_0 - T^*) - \alpha\beta t + \frac{\alpha\beta}{SK}(1 - e^{-SKt}) + (P_0 + \psi_o^* + \beta(T_0 - T^*) - \psi_s)e^{-SKt} \quad [33]$$

For an osmotic tensiometer, the pressure lag PL_{OT} is defined as

$$PL_{OT} = |P + \psi_o - \psi_s| \quad [34]$$

If the system is initially at equilibrium ($\psi_s = P_0 + \psi_{o,0}$), PL_{OT} is given by

$$PL_{OT} = \left|\frac{\alpha\beta}{SK}(1 - e^{-SKt})\right| \quad [35]$$

The response of the osmotic tensiometer to a varying temperature is thus a function of the products $\alpha\beta$ and SK.

Case 4. Osmotic Tensiometer Behavior with Sinusoidally Changing Temperature

If α is not a constant, but changes in time (e.g., due to the diurnal temperature variation), Eq. [28] cannot be solved directly. However, an analytical solution can be found if the temperature is assumed to change sinusoidally according to

$$T = T_0 + a \sin bt \quad [36]$$

Here T_0 is not only the initial temperature, but the average temperature as well. The diurnal cycle is described by a value of $b = 2.315 \times 10^{-5}\ \pi$ s^{-1}. The maximum temperature variation from T_0 is given by a; e.g., $a = 5$°C. Substitution of Eq. [36] in [30] results in

$$\frac{dP}{dt} = -SK[P + \psi_o^* + \beta(T_0 + a \sin bt - T^*) - \psi_s] \quad [37]$$

Integration of Eq. [37] with initial condition $P|_{t=0} = P_0$ results in

$$P(t) = P_0e^{-SKt} - [\psi_o^* + \beta(T_0 - T^*) - \psi_s](1 - e^{-SKt}) - \frac{SK\beta a}{[b^2 + (SK)^2]}(be^{-SKt} - b \cos bt + SK \sin bt) \quad [38]$$

Case 5. Osmotic Tensiometer with Arbitrary Temperature Changes

If α does not depend in a straightforward manner on time, then analytical solutions are hard to find, and a numerical technique is necessary to describe the evolution of pressure P. This technique is described in Materials and Methods. The results of laboratory measurements with fluctuating temperatures are compared with the outcome of the numerical model in Results and Discussion.

MATERIALS AND METHODS

Osmotic Tensiometer Design

The Type OT-0-35 osmotic tensiometer (Agro Research Instruments, Wageningen, the Netherlands) consists of a ceramic filter clamped in a brass housing (Fig. 1). A Type P 12 pressure transducer (Envec Mess- und Regeltechnik GmbH, Kassel, Germany) is located parallel to the filter. The shallow cylindrical space that serves as a cell can be filled with a polymer solution through the injection point (labeled 2 on Fig. 1). A solution of 40 g polyethyleneglycol (mol. wt. = 20 kg mol^{-1}; Merck, Darmstadt, Germany) per 100 mL distilled water is used to obtain an osmotic potential of $\psi_o = -1.3$ MPa at 22.4°C, in accordance with Peck and Rabbidge (1969a). A thermistor is located behind the pressure transducer. Measurement data (pressure, temperature) are generated at constant time intervals (between 1 s and 1 h) and sent to an external data-collection unit. The pressure transducer is calibrated from 0 to 2 MPa by connecting a gas line and cylinder to the injection point. The thermistor was calibrated by submersion of the osmotic tensiometer in a thermostatic bath for the temperature range 10 to 40°C. The resolution of the calibration instruments was within a few percent.

Filter Preparation

The filter used in the osmotic tensiometer consists of an α-alumina support (3 mm thickness) with permeability L of 1.39×10^{-16} m^2, pore size of $\approx$160 nm, particle radius $r_p \approx$300 nm, and porosity ε of 40%. This permeability is $\approx$2.5 times lower than calculated with Eq. [1] because the powder particles are nonspherical and have a broad size distribution. Two membranes of γ-alumina are applied on top of this support. Each γ-alumina layer has a thickness of $\approx$2 μm, a permeability L of $\approx 9.45 \times 10^{-20}$ m^2, and a pore size of $\approx$2.5 nm. Details on the preparation of the filters can be found in De Vos and Verweij (1998). Water molecules can permeate the filter freely, but the polyethyleneglycol used in the osmotic tensiometer has a retention $R > 99\%$. The entire filter, consisting of the α-alumina support and the two membranes, has a conductance (per unit of surface area) for water flow of $K/A = 1.76 \times 10^{-11}$ m (Pa s)$^{-1}$, which can be calculated from Eq. [10] ($\eta_{water} = 8.9 \times 10^{-4}$ Pa s at 298 K). The above values for conductance K and permeability L were measured in a liquid permeation set-up in which the steady-state flow of water through the filter material is measured as a function of the pressure difference over the filter (ΔP up to 2 MPa). The retention, R, is measured in this apparatus as well by adding polymer to the water on the high pressure side and measuring the polymer concentration on the high and the low pressure sides (c_{high} and c_{low}). Retention is given by

$$R = \left(1 - \frac{c_{low}}{c_{high}}\right) \cdot 100\% \qquad [39]$$

Laboratory Set-Up

All experiments were done in a laboratory climate chamber in which the external soil potential remained constant while the temperature changes of the laboratory were passed on directly to the tensiometer. This climate chamber consisted of a simple glass or plastic measurement cylinder ($\approx$33 cm height, $\approx$4 cm diam.) filled with $\approx$10 mL of an aqueous solution. The osmotic tensiometer was suspended over or placed directly in the aqueous solution without contact with the walls of the cylinder. The cylinder was sealed off from the laboratory atmosphere by an air-tight polymeric Parafilm (American National Can, Neenah, WI), and only the data line to the computer made a connection with the osmotic tensiometer. In this work, the aqueous solution always consisted of pure distilled water, thereby simulating a soil potential of 0 Pa. Lower soil potentials can be simulated by adding a salt to the water and using Van't Hoff's law. To prevent salts from entering the tensiometer, it is best suspended over the salt solution to create a gap for salt transfer.

Numerical Scheme

To solve the transport model for an arbitrary temperature change (Case 5), the following procedure is followed: (i) Measurement data (time t, temperature T, pressure P) are arranged column-wise in a computer worksheet program (Excel 7.0, Microsoft, Redmond, WA); (ii) The osmotic potential is determined for each time t_i, using Eq. [30], $\psi_{o,i} = \psi_o^* + \beta(T_i - T^*)$; (iii) A model prediction for P is generated using $dP/dt = -SK(P + \psi_o - \psi_s)$, which is obtained after substituting Eq. [11] and [15] in Eq. [18]. Because pure water was used to simulate the soil potential, ψ_s is set to zero. This equation can be discretized to $P_i = P_{i-1} - \Delta t \times SK(P_{i-1} + \psi_{o,i-1})$, and it can be solved with the initial conditions $P|_{t=0} = P_0$. For an accurate numerical integration, Δt must be small enough that the term $SK(P_{i-1} + \psi_{o,i-1})$ only changes slightly between each time step; formally, $|1 - (P_i + \psi_{o,i})(P_{i-1} + \psi_{o,i-1})^{-1}| \ll 1$. In the simulations a time step of $\Delta t = 60$ s is used, which gives a value for the criterion of $\approx$0.002, which is much smaller than unity.

RESULTS AND DISCUSSION

In this section two main issues are covered. First, the equations describing osmotic tensiometer behavior for an arbitrary temperature change (Case 5) are compared with the experiments described in the Materials and Methods section. Secondly, simulation results are presented that show the influence of the group SK on the behavior of the tensiometer in more detail.

Model vs. Experiment

The model outcome was compared with experiments by plotting the pressure as a function of the temperature, instead of plotting both as a function of time as is usually done. In this manner the pressure lag can be read from the graph with ease. Measured (P,T) points for three days are given in Fig. 4. The highest temperatures correspond to measurements at the end of the afternoon, while the lowest temperatures correspond to measurements around sunrise.

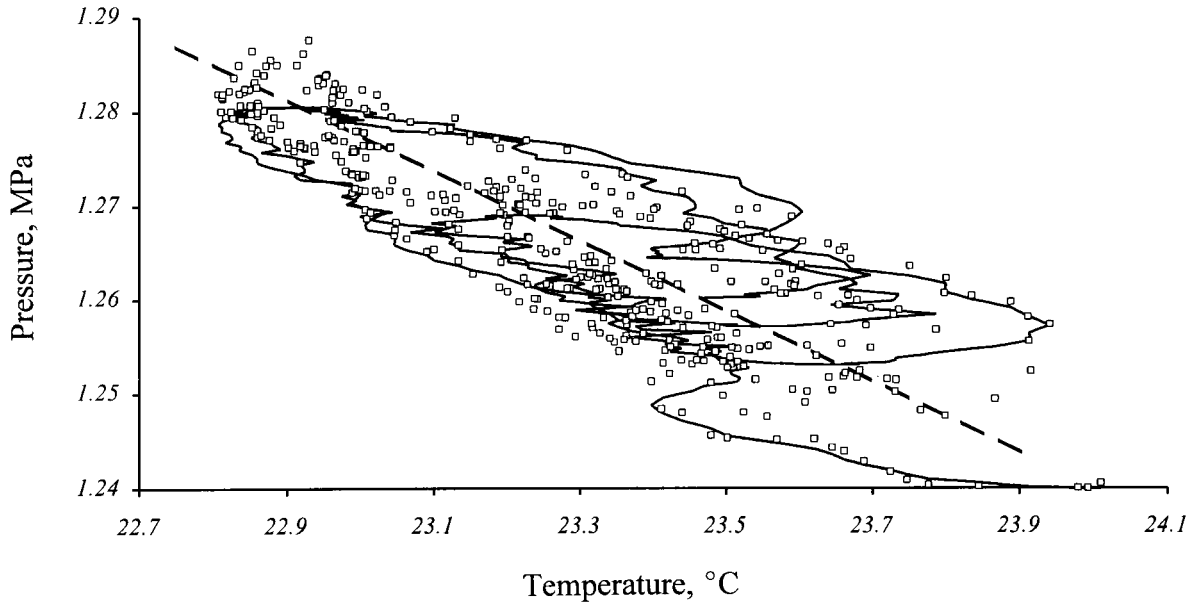

Fig. 4. Experiment (dots) vs. model (solid line) for an osmotic tensiometer submersed in free water for 3 d. Model and measurements start at T = 24°C and P = 1.24 MPa and they make three loops in clockwise direction. The dashed line gives the absolute value of the osmotic potential.

The osmotic potential, ψ_o, is assumed to depend linearly on temperature. Because soil potential is zero in the present paper, $|\psi_o|$ runs as a straight line through the measurement points in Fig. 4. The pressure lag PL_{OT} can now be read from Fig. 4 as the distance in vertical direction between a (P,T) point and the $|\psi_o|$-line.

The model described the measurements best for $\beta = 3.75 \times 10^4$ Pa K^{-1}, a reference osmotic potential of $\psi_o = -1.3$ MPa at $T^* = 22.4$°C and $SK = 1 \times 10^{-4}$ s^{-1}. The initial value was $P_0 = -\psi_{o,0} = 1.24$ MPa at $T_0 = 24$°C. The agreement between the measurements and the model is quantified in a parity plot, which shows the calculated pressure from the model as a function of the measured pressure (Fig. 5). The error is given by the distance in vertical direction between a point and the 1:1–line and is always <7 kPa (relative error < 1%).

The osmotic tensiometer filter has a surface area A of 2.01×10^{-4} m^2, which gives a value for the conductance of $K = 3.54 \times 10^{-15}$ m^3 s^{-1} Pa^{-1} (see Materials and Methods). From the above value for SK, the sensitivity is now calculated as $S = 2.82 \times 10^{10}$ Pa m^{-3}.

This value could not be compared with separate experiments, because we have yet no means to do so (see Conclusions); however, it can be compared with other data.

- Klute (1986) gives a value of $S = 3.10^{12}$ Pa m^{-3} for a Validyne DP-50 pressure transducer (Validyne Engineering, Northridge, CA) and Towner (1980) uses $S = 1 \times 10^{12}$ Pa m^{-3} as a typical value for a tensiometer under tensiometer-limited conditions.
- The local indent at the center of a Druck 800-series pressure transducer was measured by the manufacturer as $w_{r=0} = 0.665$ μm (A.P. Van Loon, personal communication, 1997) for a pressure difference of 2 MPa for a transducer made of silicium ($E = 1.07 \times 10^{11}$ Pa, $\nu = 0.33$) with dimensions $\delta_t \approx 178$ μm and $R \approx 1.5$ mm. Equation [12] predicts $w_{r=0} = 2.8$ μm, which is of the same order as the measurement, which is a satisfactory first estimate. Equation [14] predicts a sensitivity of $S = 3.0 \times 10^{17}$ Pa m^{-3} for this transducer.

These three values are higher than the value determined in our experiments. This may be due to the choice of transducer or to differential expansion of the brass tensiometer housing and/or ceramic filter that is caused by the changing pressure and temperature. Besides, it is possible that the value for conductance K was overestimated because other resistances to water flow exist besides the filter resistance. In that case, the above calculation would underestimate the sensitivity, S.

By measuring the vertical distance between a measured (P,T) point and the dashed $|\psi_o|$-line, a pressure lag PL_{OT} is found in the range of 7 to 11 kPa. For soil potentials below −100 kPa, this pressure lag results in a

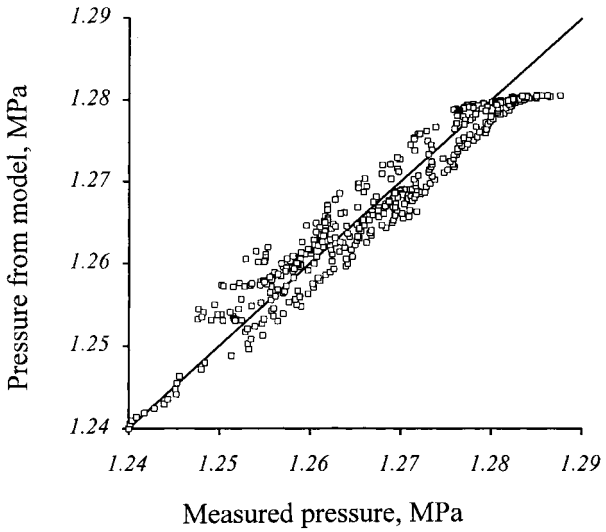

Fig. 5. Parity plot showing the agreement between the model and the experiments of Fig. 4.

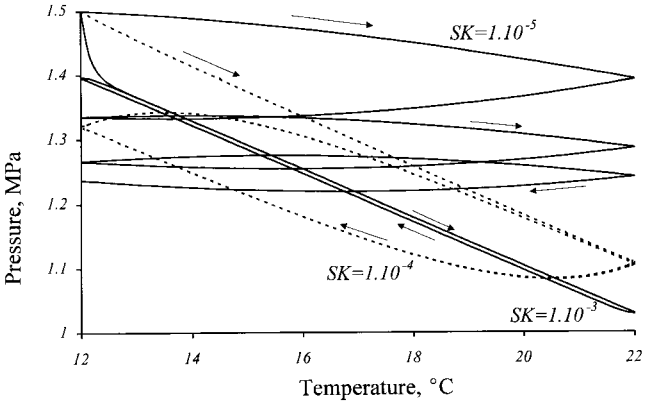

Fig. 6. Influence of the group *SK* on the pressure response curves for the osmotic tensiometer. The absolute value of the osmotic potential $|\psi_o|$ is a straight line starting at T = 12°C and P = 1.4 MPa with a gradient of $-\beta = 3.75 \times 10^4$ Pa K^{-1}.

measurement error of <10%, which may be acceptable. Note that the pressure lag followed from a diurnal temperature change in our laboratory of only one degree. In the next section the pressure lag is modelled for an outdoor situation in which the temperature difference between sunrise and sunset is 10°C.

Further Evaluation of the Model

Model runs were made with a constant change of temperature during day and night ($\alpha_d = -\alpha_n$ = 10°C/12 h = 2.31×10^{-4} K s^{-1}) for $\beta = 3.75 \times 10^4$ Pa K^{-1}, $\psi_o = -1.4$ MPa at T^* = 12°C, a starting value P_0 = 1.5 MPa at T_0 = 12°C, a soil potential ψ_s of zero, and a time-step Δt = 600 s. For three values of the product *SK* the results for the first three days are summarized in Fig. 6. Here, the temperature starts to increase from 12°C at 0600 h (sunrise) and reaches a maximum of 22°C at 1800 h (sunset). At that moment it again starts to decrease, ultimately to arrive at the value of 12°C the next morning. The osmotic potential changes linearly from −1.4 MPa at sunrise to −1.05 MPa at sunset.

For $SK = 1 \times 10^{-3}$ s^{-1} the pressure lag PL_{OT} goes down to 3.5 kPa within 1 h and remains at that value. Only for a few minutes around 0600 h and in the evening at 1800 h, is the pressure lag lower. For $SK = 1 \times 10^{-4}$ s^{-1}, the pressure lag increases during day and night until a maximum of ≈80 kPa at sunrise and at sunset. For $SK = 1 \times 10^{-5}$ s^{-1}, osmotic tensiometer performance is poor. After 3 d the pressure curve has almost come to a stationary situation ≈1.24 MPa. The lowest values of the pressure lag are now found around midnight and noon. Around sunrise and sunset the pressure lag is ≈0.2 MPa.

CONCLUSIONS

The basic features of the osmotic tensiometer are described in a transport model that incorporates filter permeability *K*, sensitivity *S*, differential temperature change α, and osmotic pressure–temperature gradient β. These parameters can be derived from separate experiments or auxiliary models. In the transport model, osmotic tensiometer response behavior is described by the products αβ and *SK* and is described with reasonable accuracy for experiments in a laboratory climate chamber. Further experimental validation of the model, however, is still necessary and is currently done with the following techniques: (i) independent measurements of the influence of the temperature on the osmotic potential; e.g., by using the osmotic tensiometer in a climate chamber at a constant temperature until equilibrium is established to accurately determine the $\psi_o(T)$ function; (ii) measurement of the response behavior of the osmotic tensiometer for different polymer concentrations and temperature changes.

The independent measurement of the sensitivity of the transducer remains a problem. To determine the sensitivity it would be necessary to measure the indent of the transducer by some optical method while a pressure difference is applied.

The model can be extended to describe the transfer of mass (e.g., salt movement through the filter, polymer diffusion within the cell) and heat (e.g., heating and cooling of the osmotic tensiometer and its influence on the expansion of the housing and the cell solution).

ACKNOWLEDGMENTS

This work is supported financially by the Dutch Science Foundation (NWO/STW). The authors thank H. Kruidhof and C. Huiskes (Inorganic Materials Sci., Univ. of Twente), A.H. van den Boogaard (Mechanical Engineering, Univ. of Twente) and C. Dirksen (Wageningen Univ.) for their help in the conceptual design of the osmotic tensiometer, in the filter preparation, and for useful discussions in preparation of the manuscript. Special thanks go to A.P. van Loon (Agro Research Instruments, Wageningen) for the design and construction of the osmotic tensiometer.

REFERENCES

Alami-Younssi, S., A. Larbot, M. Persin, J. Sarrazin, and L. Cot. 1995. Rejection of mineral salts on a gamma alumina nanofiltration membrane. Application to environmental process. J. Membrane Sci. 102:123–129.

Bird, R.B., W.E. Stewart, and E.N. Lightfoot. 1960. Transport phenomena. John Wiley & Sons, New York.

Bocking, K.A., and D.G. Fredlund. 1979. Use of the osmotic tensiometer to measure negative pore water pressure. Geotech Test. J. 2:3–10.

Campbell, G.S., and W.H. Gardner. 1971. Psychrometric measurements of soil water potential: Temperature and bulk density effects. Soil Sci. Soc. Am. Proc. 35:8–12.

De Vos, R.M., and H. Verweij. 1998. High-selectivity, high-flux silica membranes for gas separation. Science 279:1710–1711.

Dullien, F.A.L. 1979. Porous media, fluid transport and pore structure, Academic Press, New York.

Guan, Y., and D.G. Fredlund. 1997. Use of the tensile strength of water for the direct measurement of high soil suction. Can. Geotech. J. 34:604–614.

Haise, H.R., and O.J. Kelley. 1950. Cause of diurnal fluctuations in tensiometers. Soil Sci. 70:301–313.

Klute, A., and W.R. Gardner. 1962. Tensiometer response time. Soil Sci. 93:204–207.

Klute, A. (ed.) 1986. Methods of soil analysis. Part 1. Physical and mineralogical methods. 2nd ed. Agron. Monogr. 9. SSSA and ASA, Madison, WI.

Liu, H.H., and J.H. Dane. 1993. Reconciliation between measured and theoretical temperature effects on soil water retention curves. Soil Sci. Soc. Am. J. 57:1202–1207.

Mulder, M. 1991. Basic principles of membrane technology. Kluwer Academic Publ. Dordrecht, the Netherlands.

Peck, A.J., and R.M. Rabbidge. 1966. Soil-water potential: Direct measurement by a new technique. Science 151:1385–1386.
Peck, A.J., and R.M. Rabbidge. 1969a. Design and performance of an osmotic tensiometer for measuring capillary potential. Soil Sci. Am. Proc. 33:196–202.
Peck, A.J., and R.M. Rabbidge. 1969b. Methods and means for measuring the free energy of solvents. U.S. Patent 3 455 147.
Richards, L.A., M.B. Russell, and O.R. Neal. 1937. Further developments on apparatus for field moisture studies. Soil Sci. Soc. Am. Proc. 2:55–64.
Richards, L.A. 1949. Methods of measuring soil moisture tension. Soil Sci. 68:95–112.
Towner, G.D. 1980. Theory of time response of tensiometers. J. Soil Sci. 31:607–621.
Vinson, J.R. 1974. Structural mechanics: The behavior of plates and shells. John Wiley & Sons. New York.
Watson, K.K., and R.D. Jackson. 1967. Temperature effects in a tensiometer–pressure transducer system. Soil Sci. Soc. Am. Proc. 31:156–160.

Errors of Dual Thermal Probes Due to Soil Heterogeneity across a Plane Interface

J. R. Philip and G. J. Kluitenberg*

ABSTRACT

The dual thermal probe enables estimation of the thermal diffusivity, volumetric heat capacity (*C*), and thermal conductivity of soils. It has been much employed for moisture estimation because of the strong dependence of *C* on soil water content. The present study investigates the effectiveness of dual probes near heterogeneities. Exact solutions are found for four probe/soil configurations involving heterogeneity. In one configuration the heating probe is on the plane interface between different soils. For the three other configurations it is located close to three different discontinuities: near a soil surface and outside, and behind, a wetting front. Heterogeneity errors are found to be small provided the heterogeneity is no closer to the probes than probe separation (typically 0.006 m). Estimates of *C* may provide good resolution of soil water content in critical regions such as near surfaces and fronts.

The dual-probe heat pulse method for measuring soil volumetric heat capacity was proposed by Campbell et al. (1991). Because of the direct relation between soil heat capacity and volumetric moisture content, dual thermal probes offer means of estimating soil water content (Bristow et al., 1993; Tarara and Ham, 1997; Bremer et al., 1998; Bristow, 1998; Song et al., 1998). Dual probes also enable estimates of soil thermal diffusivity and conductivity (e.g., Kluitenberg et al., 1993; Bristow et al., 1994; and Kluitenberg et al., 1995). Kluitenberg et al. (1993, 1995) investigated the errors that were incurred in the simplified analysis (Campbell et al., 1991) in which the probes are treated as infinite and heat input as an instantaneous line source.

These various studies have left unexamined the question of dual-probe error due to heterogeneity, such as spatial variation of soil thermal properties. We have in mind not only variation of intrinsic soil properties, but also of moisture content within a homogeneous soil. We observe, further, that the various theoretical analyses treat the dual probe as embedded in an infinite soil mass. This assumption cannot be valid, for example, when the probes are located very close to the soil surface. Propinquity to the surface is, from this viewpoint, one more form of heterogeneity. The greatest fluctuations of soil moisture, and hence of thermal properties, occur at and near the soil surface. The question of the performance of dual probes close to the surface is therefore of considerable interest and practical importance. Because of their small size, dual probes may be useful near heterogeneities; but it is clearly desirable to test this expectation.

In the present study we develop exact solutions for four probe/soil configurations involving heterogeneity. We limit our analyses to the simple model of Campbell et al. (1991) with infinite probe lengths and the heat pulse an instantaneous line source. Introducing the complications of the nonzero radius and finite length of the probes, and the nonzero duration of the heat pulse, would leave unaffected the order of magnitude of the errors arising from heterogeneity. Kluitenberg et al. (1993) have shown that these complications cause only minor modifications to the simple Campbell model for typical probe geometries and heating times.

MATHEMATICAL MODELS

Heat Equation

The heat conduction equation for a soil region of uniform properties is

$$\frac{\partial T}{\partial t} = \kappa \nabla^2 T \qquad [1]$$

where T is temperature (K), t is time (s), κ is the thermal diffusivity ($m^2\ s^{-1}$), and ∇^2 the Laplacian (m^{-2}). The thermal conductivity λ ($Wm^{-1}\ K^{-1}$) and the volumetric heat capacity C ($Jm^{-3}\ K^{-1}$) are related by κ by

$$\kappa = \lambda / C \qquad [2]$$

We treat the heating probe as an instantaneous line source: infinite in length, of strength q (Jm^{-1}), released at the instant $t = 0$. The (x,z) plane is normal to the line source, which is located at $(x,z) = (0,0)$. We shall also use polar coordinates (r,ϕ) such that

$$r = (x^2 + z^2)^{1/2}, \qquad \tan \phi = z/x, \qquad -\pi \le \phi \le \pi \qquad [3]$$

The heating probe is thus at $r = 0$.

We shall examine instantaneous source solutions of Eq. [1]

J.R. Philip (deceased), CSIRO Land and Water, G.P.O. Box 1666, Canberra, ACT 2601, Australia; and G.J. Kluitenberg, Dep. of Agronomy, Kansas State University, Manhattan, KS 66506. Contribution no. 99-46-J from Kansas Agric. Exp. Stn., Manhattan, KS. Research supported by Western Regional Research Project W-188. Received 12 Aug. 1998. *Corresponding author (gjk@ksu.edu).

Published in Soil Sci. Soc. Am. J. 63:1579–1585 (1999).